Characterization and Chemical Properties of Pd−Au Alloy Surfaces†

Tao Wei, Jinhai Wang, and D. Wayne Goodman*

Department of Chemistry, Texas A&M University, College Station, Texas 77842-3012

Received: October 31, 2006; In Final Form: January 11, 2007

The chemisorptive behavior of CO on Pd−Au alloy films has been studied by infrared reflection−adsorption spectroscopy (IRAS). Geometric (ensemble) and electronic (ligand) effects have been addressed by comparing the results with the corresponding single-component systems. A unique CO vibrational feature at 2088 cm^{-1} is associated with CO adsorption on isolated Pd sites. Considering the frequency of the CO stretching mode, these data support mainly an influence of an ensemble effect on the chemical properties and contradict any significant contribution from a ligand effect. The surface concentration of isolated Pd sites can be controlled systematically by altering the bulk Pd−Au alloy composition, thus providing a method for studying isolated Pd as an active site for various catalytic reactions.

1. Introduction

Alloying is used widely to alter the chemical properties of metal surfaces, since the catalytic properties of alloys are often remarkably different from those of the single-metal-component catalyst.[1−4] The prospect of making novel catalysts with improved properties has led to a continuing interest in the surface chemistry of alloys. Pd−Au is particularly important because of its use in several important industrial reactions including vinyl acetate synthesis.[5−7]

Early studies on Pd−Au alloys have addressed primarily two types of model systems: stable bulk alloys and thin film surface alloys prepared by deposition of one metal onto a single crystal of the other (for example, deposition of Pd onto a Au(111) surface or vice versa). However, these studies have been limited because of the difficulties in the preparation and the control of the surface alloy compositions. To avoid this difficulty, we have prepared Pd−Au alloy films by depositing the two metals onto a third metal substrate, Mo(110).[8] Since both Pd and Au have limited solubilities in Mo(110), a stable alloy film is formed upon annealing. Previous low-energy electron diffraction (LEED) studies have shown that pseudomorphic, fcc<111>-like surfaces are formed when multilayer Pd or Au is grown on Mo(110).[9−13] Accordingly a mixed Pd−Au film can be anticipated to form a structure with a <111>-like surface. Besides the flexibility in the variability of the Pd to Au bulk ratio, this alloy preparation scheme is very convenient with respect to film preparation and surface cleanliness. In order to minimize any complications associated with the Mo substrate, relatively thick films (10 monolayers or greater) are used.[69]

The surface composition, morphology, and electronic structure of Pd−Au model catalysts have received extensive attention in the literature. Strong surface segregation of Au has been observed by Auger electron spectroscopy (AES), low-energy ion scattering spectroscopy (LEISS), and scanning tunneling microscopy (STM).[14−20] With the use of electronic spectroscopic methods, i.e., X-ray photoelectron spectroscopy (XPS), X-ray absorption near-edge spectra (XANES), and ultraviolet photoelectron spectroscopy (UPS), the net charge transfer from Pd to Au was found to be very small due to electron redistribution or orbital rehybridization.[21−23] Several studies have shown that the anneal temperature and length are crucial to determining the alloy surface morphology and composition; typically, relatively high annealing temperatures smooth the surface and lead to enrichment of the surface in the more stable surface component.[8,24−26] In addition, ensemble effects have been purposed to play a dominant role in the enhancement of catalytic reactivity for several reactions.[24,27−29]

Vibrational studies of the chemisorptive properties of Pd−Au alloy surfaces are limited. Kugler and Boudart investigated carbon monoxide adsorption on a series of silica-supported, high-surface-area Pd−Au alloy catalysts using infrared spectroscopy. The goal of these authors was to examine the relative importance of ensemble and ligand effects in this system; however, broad IR features caused by the variability of particle sizes and morphologies made definitive interpretation difficult.[30] To further explore this aspect of alloying, we have carried out a similar study for a planar Pd−Au alloy catalyst using infrared reflection adsorption spectroscopy (IRAS). Since CO adsorption on low-index Pd and Au single-crystal surfaces has been extensively studied,[31−39] comparison of the vibrational spectra enables the acquisition of more detailed information regarding the chemical properties of Pd−Au alloy surfaces.

2. Experimental Section

This study was carried out in a UHV chamber with a base pressure of 1.0×10^{-10} torr. The chamber was equipped with an Auger electron spectrometer, a quadrupole mass analyzer for temperature-programmed desorption (TPD), and an infrared cell separated from the main chamber by a sliding seal. This apparatus has been described in detail elsewhere.[38,40−43] The infrared cell was fitted with flange-mounted CaF_2 windows in the infrared beam path. IRAS spectra were collected using a Mattson Cygnus 100 spectrometer in the single-beam mode with external optics aligned for an incident angle of 85° from the sample normal. Detection was via a liquid-nitrogen-cooled MCT detector; all spectra are averages of 512 scans at 4 cm^{-1} resolution. Approximately 4.5 min was required to acquire each spectrum.

† Part of the special issue "Kenneth B. Eisenthal Festschrift".

* To whom correspondence should be addressed. E-mail: Goodman@mail.chem.tamu.edu.

10.1021/jp067177l CCC: $37.00
Published on Web 02/14/2007

The Mo(110) single crystal was mounted on the sample probe with a tantalum wire spot-welded around the edge of the sample. A type C thermocouple (W−5%Re/W−26%Re, H. Cross Co.) was used to monitor the sample temperature. This assembly allowed resistive heating to 1500 K and liquid nitrogen cooling to ~80 K. The Mo(110) sample was cleaned by oxidation (1200 K, 1×10^{-7} torr O_2) and heating to 2100 K until no carbon and oxygen were detectable by AES.

The Pd, Au dosers were constructed by wrapping high-purity metal wires around a tungsten wire. Impurities were removed by thoroughly degassing before dosing. All metal depositions were performed with the sample at room temperature. The dosing rates were calibrated by TPD. Carbon monoxide and oxygen (99.99%, Matheson Gas Products) were further purified by fractional condensation and transferred to glass bulbs attached to the gas manifold.

3. Results and Discussion

CO Adsorption on Pd and Au Monometallic Films. Control experiments on monometallic Pd and Au films were first carried out to provide a reference for the Pd−Au alloy studies. Because of the high surface free energy and dense packing of Mo(110), fcc metals have been shown to grow layer-by-layer with a smooth, <111> orientation.[9−13,44] Accordingly the vibrational spectra of CO adsorbed on a relatively thick Pd film is anticipated to be comparable to CO adsorbed on Pd(111). The coverage-dependent surface structures of CO overlayers on Pd(111) have been identified by various surface science techniques.[31,32,35,45,46] Vibrational spectroscopy, in particular the C−O stretching frequency, has been used to assign adsorption sites.[31,32] On the basis of these studies, up to a CO coverage of 0.33 monolayers (ML), the $(\sqrt{3} \times \sqrt{3})R30°-1CO$ structure is the dominant phase, where CO resides primarily on 3-fold hollow sites. This structure yields a distinctively low C−O vibrational frequency of ~1850 cm^{-1}. Increasing the CO coverage to 0.50 ML results in a new overlayer phase, the $c(4 \times 2)-2CO$ structure, where CO populates either the bridging sites or 3-fold hollow sites.[45] This structure corresponds to a C−O stretching frequency of ~1920 cm^{-1}. Within the CO coverage range of 0.5−0.75 ML, various complex overlayer structures with CO mainly on bridging sites have been reported, with a CO vibrational band near 1965 cm^{-1}. Finally upon reaching saturation at a CO coverage of 0.75 ML, the adsorbate structure transforms to a $(2 \times 2)-3CO$ phase, with CO occupying both atop and 3-fold hollow sites with vibrational features at 2110 and 1895 cm^{-1}, respectively. A phase diagram showing a transition between these CO overlayer structures at various temperatures and pressures has been reported by Ozensoy et al. based on IRAS data.[33,48]

Figure 1 shows an IRAS annealing series for a 10 ML Pd film on Mo(110) in a 5×10^{-8} torr CO background pressure. The spectra are independent of the direction of the temperature change, provided that the film is annealed to 600 K in a CO background. At a sample temperature of 450 K, a broad feature at 1845 cm^{-1} is first observed and can be attributed to CO bound primarily at 3-fold hollow sites. As the sample is cooled and the CO equilibrium coverage is increased, this broad feature sharpens and shifts continuously to a higher frequency at 1962 cm^{-1}, consistent with a more ordered adsorbate superstructure in which the bridging sites are primarily occupied. Below 200 K, a prompt change in the spectrum is apparent. Two new, sharp features grow in at 2109 and 1892 cm^{-1}, while the intensity of the bridging CO peak decreases gradually. This spectral evolution corresponds with a transition of CO from bridging sites to a combination of atop and 3-fold hollow sites. Besides these well-defined and intense bands, a weak feature at 2086 cm^{-1} is evident in the temperature range of 300−200 K with no apparent frequency shift. This feature is assigned to a small amount of CO adsorbed onto Pd atop sites, possibly due to a slight disorder in the CO overlayer or a mismatch between the compressed CO $c(4 \times 2)$ overlayer and the Pd(111) substrate that forces some CO onto atop sites.[33,34,48] Identical behavior was observed previously for studies of Pd(111) at low and elevated pressures. Finally, it is noteworthy that weak features at ~1950 and ~1990 cm^{-1} can still be detected at 80 K and saturation CO coverage. Ideally, CO only populates the Pd atop and 3-fold hollow sites at saturation coverage on Pd(111).[33,34] However, similar features have been observed by Kuhn et al.[33] and Ozensoy et al.[48] in CO ambient pressure studies on Pd(111). These features were interpreted as CO adsorption on Pd bridging sites due to a slight disorder in the $(2 \times 2)-3CO$ phase or to CO adsorption at antiphase domain boundaries.[47,48] It was also pointed out that the sample preparation conditions have a great impact on these features.[33−35,49] Less intensity in these features was detected when the sample surface was annealed in a CO background at elevated temperatures, similar to results obtained for Pd films.[50]

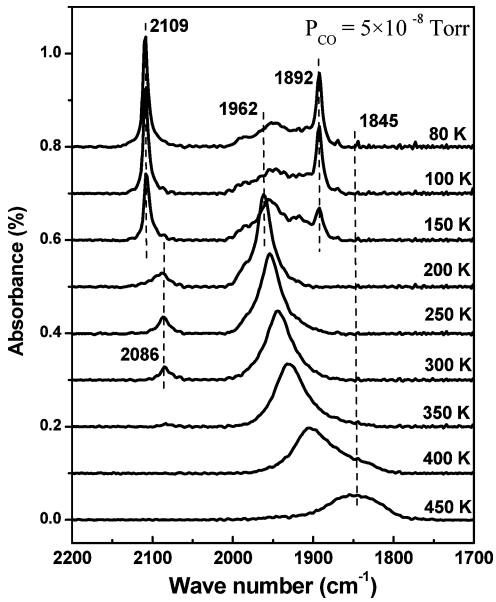

Figure 1. IRAS spectra for CO adsorption on a 10 ML Pd/Mo(110) surface as a function of temperature.

In general, the same adsorption progression and frequencies observed in studies of a 10 ML Pd film and Pd(111) single crystal clearly indicate that the 10 ML Pd film on Mo(110) consists primarily of flat, <111> facets. More importantly, the same transition temperatures between the CO adsorption sites in these studies (specifically, 400 K for 3-fold hollow sites to bridging sites and 150 K for bridging sites to atop and 3-fold hollow sites) confirm that the 10 ML Pd film has Pd bulklike properties. Very different CO adsorption properties have been reported by Xu and Goodman for a pseudomorphic Pd monolayer surface on Mo(110).[51] These authors report that the CO binding energy on monolayer Pd film is reduced by 12 kcal/mol relative to Pd(111); in contrast to the Pd(111) surface, the atop sites have a higher CO binding energy compared to that of the bridging sites. This variation was attributed to a substantial modification of the electronic structure of the Pd monolayer by the Mo(110) substrate. The similar CO adsorption behavior on the 10 ML Pd film and the Pd(111) single-crystal surface assures

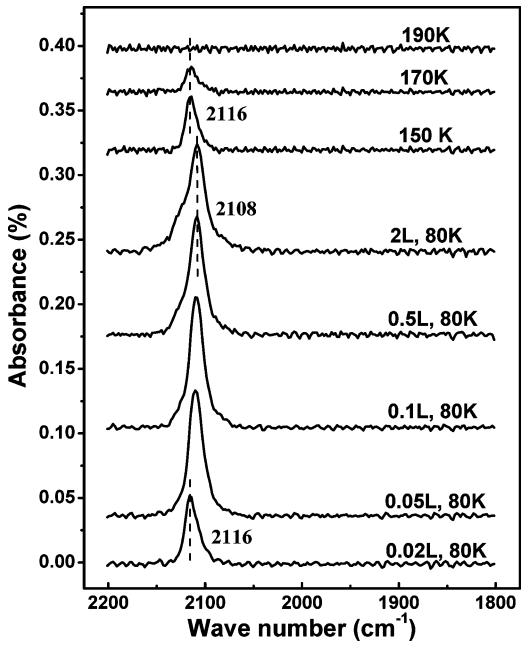

Figure 2. IRAS spectra for CO adsorption on a 10 ML Au/Mo(110) surface at the indicated exposures and temperatures.

that the 10 ML film is thick enough to eliminate any influence of the Mo substrate.

The adsorption behavior of CO on the Au surface is relatively simple compared to that of the Pd surface mainly because of the weak interaction between Au and CO. Gottfried et al. estimated a maximum CO coverage of 0.3 ML at 80 K for a Au(110)−(1 × 2) surface,[39] which is a closed-packed Au surface after the surface reconstruction. The vibrational studies from a variety of Au systems at both UHV and ambient conditions showed only one CO stretching feature at around 2110 to ∼2120 cm^{-1}, which was assigned to CO adsorption on Au atop sites.[36−38,43,52] In contrast to the Pd system, this feature red-shifts with increasing CO coverage. This abnormal shift has been found to be the case for all group IB metals and is characteristic of Au surfaces.

Figure 2 displays a series of IRAS spectra for CO adsorption on a 10 ML Au film on Mo(110) at the indicated exposures and temperatures. At the low-coverage limit, the CO absorbance is a single feature at 2116 cm^{-1}. As the exposure is increased, this feature red-shifts continuously to 2108 cm^{-1} at saturation, in close agreement with early IRAS results on Au(110)−(1 × 2) and 8 ML Au film/Mo(112).[38,52] The warming experiments show the CO desorbs completely from the surface between 170 and 190 K, in agreement with the TPD studies of Gottfried et al. on Au(110).[39] This bulklike Au behavior with respect to CO adsorption on 10 ML Au film/Mo(110) supports the use of this system as a prototype of Au(111).

CO Adsorption on Pd−Au Alloy Films. Figures 3 and 4 illustrate the coverage-dependent (Figures 3A and 4A) and temperature-dependent (Figures 3B and 4B) CO-IRAS spectra for the 5 ML Pd/5 ML Au/Mo(110) alloy system (Au deposited first) annealed at different temperatures. Note that the coverage-dependent spectra were acquired by increasing the CO exposure at a sample temperature of 80 K and the temperature-dependent spectra were collected by warming the sample to the indicated temperature in vacuum. In Figure 3, the alloy film was first annealed at 600 K for 30 min prior to the CO adsorption. Within the low CO dosage regime (<0.1 L), three apparent features, at 2103, 2078, and 1940 cm^{-1}, intensify simultaneously (Figure 3A). All these bands show no frequency shift with further CO exposure. When CO saturates the surface, the IRAS spectrum is dominated by a feature at 2078 cm^{-1} and a shoulder at 2103 cm^{-1}. These frequencies are typical for linearly bound CO on metal surfaces. According to the temperature-dependent spectra (Figure 3B), the shoulder at 2103 cm^{-1} disappears at a lower temperature (between 150 and 200 K), indicating a weaker CO adsorption species. Hence, this shoulder can be attributed to CO residence on Au atop sites. It is noteworthy that the Au-related feature is already visible in these spectra. Since Au was covered by 5 ML Pd during the film preparation, these data imply that the Pd and Au intermix extensively after annealing at 600 K. This is consistent with data of Shih et al. for the Pd/Au(111) alloy system using AES and LEED techniques[53] that surface alloying between Pd and Au occurs at room temperature and with complete alloying at 550 K. A broad band at 1940 cm^{-1} is also evident at CO saturation coverage with features assigned to CO population on the Pd 2-fold bridge and 3-fold hollow sites. Both the Pd-related features (an atop feature at 2078 cm^{-1} and a multiply bound feature at 1940 cm^{-1}) are found to be much broader than those in the corresponding Pd single-crystal system, suggesting that CO adsorption sites on this alloy surface are not well ordered. The absolute IR intensities in these spectra are also largely attenuated in comparison with single-crystal cases, implying that a large fraction of the CO adsorbs on this alloy surface with bonding angles significantly aligned from the surface normal. Furthermore, both the asymmetrical peak shape (a low-frequency tail) and the simultaneous growth of three features at the low CO coverage denote limited CO mobility on this surface.[31] All these observations suggest that the alloy surface is relatively rough after annealing at 600 K.

The same alloy film was further annealed at 800 K for 45 min to obtain the IRAS measurements shown in Figure 4, where substantial changes are apparent in the spectra. The broad peak observed in the previous experiment at 1940 cm^{-1} completely disappears at all CO coverages with only a single feature at 2088 cm^{-1} following a low CO exposure (Figure 4A). With additional CO dosage, a second peak emerges at 2112 cm^{-1}, well resolved from the 2088 cm^{-1} peak, and is assigned to CO adsorption on Au atop sites based on the thermal behavior of this peak (Figure 4B). The full width at half-maximum (fwhm) of the Pd atop feature at 2088 cm^{-1} is 7 cm^{-1}, comparable with that from a Pd single-crystal surface. Moreover, the IR intensities are greatly enhanced. It may be inferred that the alloy surface is smooth and well ordered after annealing at 800 K. The thermally induced change in morphology has been reported in numerous early studies. For instance, Gleich et al. carried out a STM study on the Au/Pd(111) alloy system, and showed that a flat alloy surface with no islands on the terraces can only be obtained by annealing at 925 K.[25] Baddeley et al. studied the inverse system (Pd/Au(111)) using STM and observed that annealing at 550 K restores a roughened, Pd overlayer to an atomically flat alloy surface.[24] Similar results have been observed for Pd−Cu alloy systems.[54,55] Therefore, the substantial differences in our IR spectra with different annealing temperatures can be rationalized by the associated morphological changes. It is interesting to note that alloying (intermixing) occurs at a lower temperature than does surface smoothing.

It should also be mentioned that our CO vibrational frequency assignments are consistent with previous high-resolution electron energy loss spectroscopy (HREELS) studies. Sellidj and Koel investigated the Pd/Au(111) alloy system and reported two energy losses at 1910 and 2090 cm^{-1} at saturation CO coverage, features attributed to CO on Pd 2-fold bridging and atop sites.[56] Behm and co-workers studied the inverse system (Au/Pd(111))

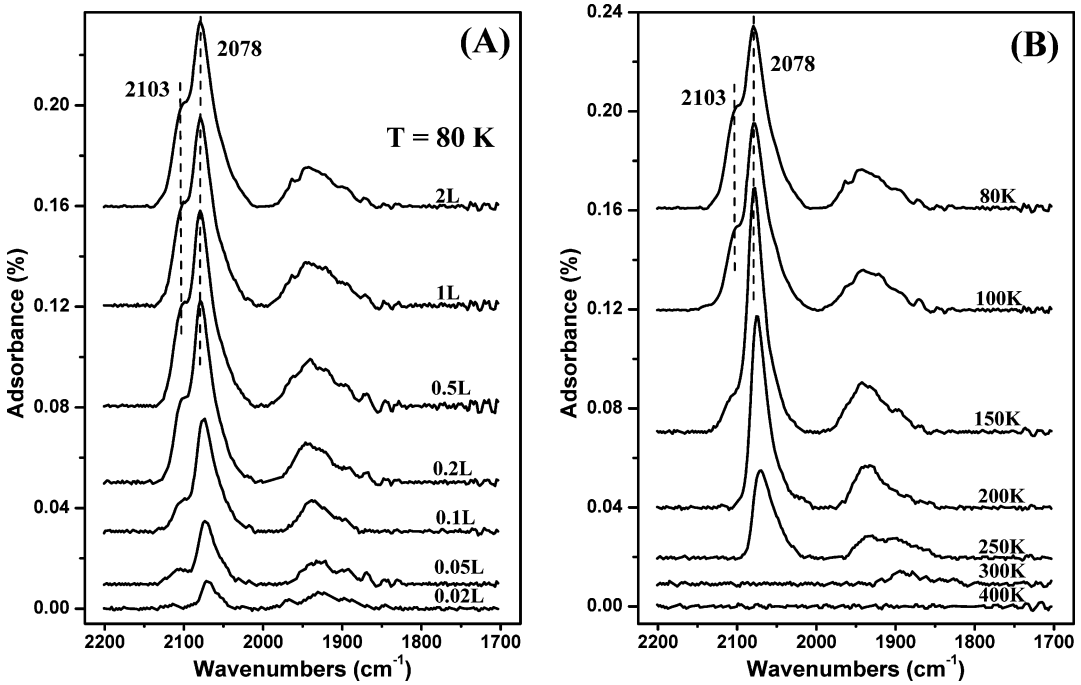

Figure 3. Coverage-dependent (A) and temperature-dependent (B) IRAS spectra for CO adsorption on the 5 ML Pd/5 ML Au/Mo(110) system. The alloy film was annealed at 600 K for 30 min.

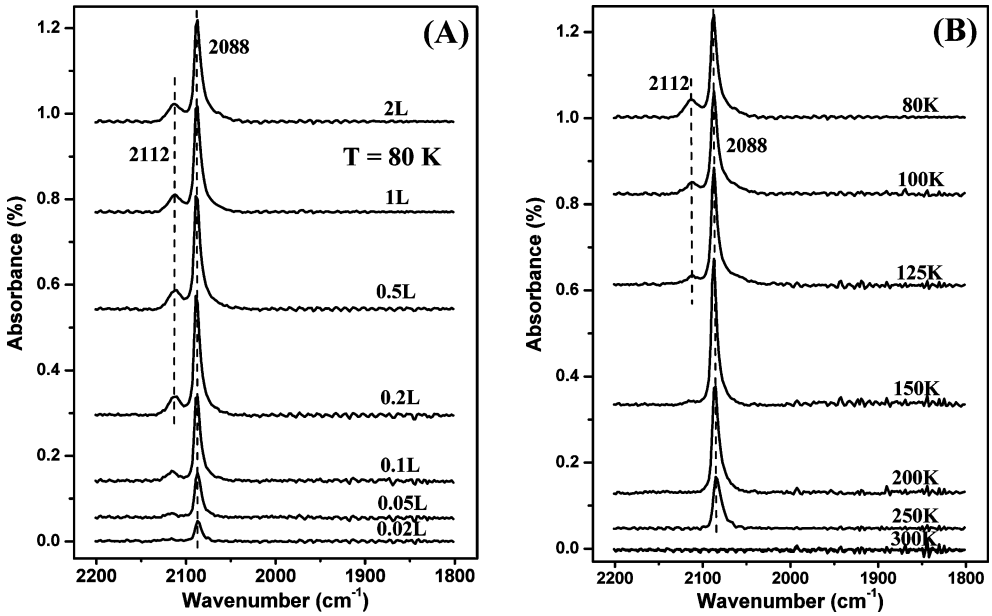

Figure 4. Coverage-dependent (A) and temperature-dependent (B) IRAS spectra for CO adsorption on the 5 ML Pd/5 ML Au/Mo(110) system. The alloy film was annealed at 800 K for 45 min.

and observed energy loss features at 237−240, 258, and 263 meV (1920−1944, 2090, and 2130 cm^{-1}). These authors assigned these losses to CO adsorption on small patches of Pd, Au-coordinated Pd atoms, and Au atop sites.[25,57] However, due to the relatively low resolution of HREELS, differentiating the features among the Au atop sites, Pd atop sites, and Au-coordinated Pd sites was not possible. Thus, a systematic investigation of the frequency shift induced by the ligand (electronic) effect has not been made to date.

Alloying Effect. The term "alloying effect" refers to the promotion of catalytic properties with the addition of a second metal component to a single-metal catalyst and is often explained on the basis of ensemble (geometric) and ligand (electronic) effects. The ensemble effect refers to the formation of a special arrangement of several reactive metal atoms, which makes the desired chemisorption bonds preferable. The ligand effect describes electronic modifications resulting in heteronuclear metal−metal bonds, leading to optimal chemisorption bonding between the reactive metal atom and an adsorbate. IRAS using CO as a probe molecule has been shown to be an effective technique for investigating alloying effects.[28,30] In particular, the presence or absence of characteristic CO stretches can be used to monitor adsorption sites on the surface, providing insight into the ensemble effect. The CO vibrational frequency shift can be used to identify the changes in the interactions between the substrate and CO molecules, which reflect the electronic modifications of the substrate surface induced by the second metal (the ligand effect).

In Figure 5, IRAS spectra for 10 ML Pd film, 5 ML Pd/5 ML Au alloy film (annealed at 800K), and 10 ML Au film at

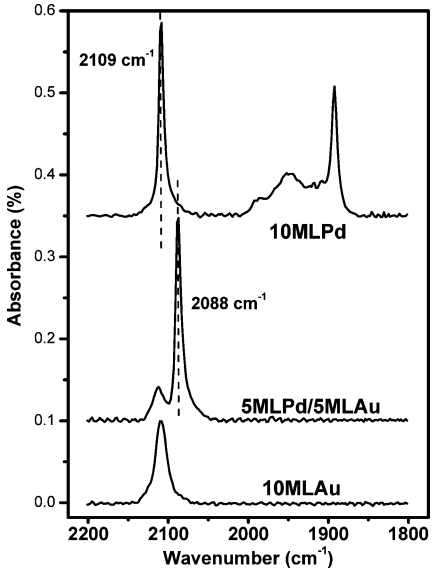

Figure 5. Comparison of IRAS spectra for CO adsorption on the 10 ML Pd film, 5 ML Pd/5 ML Au alloy film, and 10 ML Au film on Mo(110) at saturation CO coverage. The alloy film was annealed at 800 K for 45 min, and the spectra were acquired at 80 K.

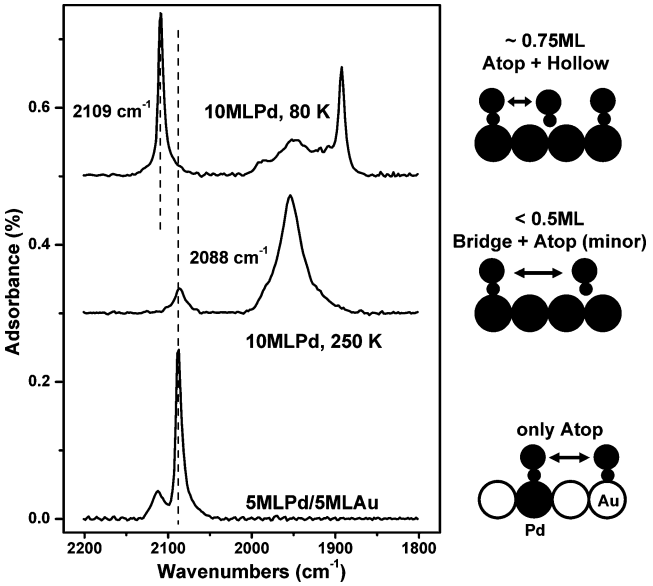

Figure 6. IRAS spectra for CO adsorption on the 10 ML Pd film and 5 ML Pd/5 ML Au alloy film on Mo(110). The top and middle spectra were collected in the 5×10^{-8} torr CO background at the indicated temperatures. The bottom spectrum corresponds to saturation CO coverage at 80 K. On the right are schematic side views of CO adsorption models for each surface.

saturation CO coverage of 80 K are compared. It is apparent that the Pd multifold features (2-fold bridge and 3-fold hollow features) are completely eliminated on the alloy surface, suggesting the Pd atop sites are the only accessible adsorption sites on the 5 ML Pd/5 ML Au alloy surface. As the stronger bonding sites, the Pd multisite bonding features have been observed in Pd single-crystal and oxide-supported Pd cluster surfaces.[31,32] Hence, their absence indicate that contiguous Pd atoms are not present on the surface, i.e., only isolated Pd sites or singleton Pd species are present. This result can be understood in view of earlier studies. Sadigh et al. obtained atomic STM images for Pd−Au monolayer films on Ru(0001) and demonstrated the presence of pronounced chemical short-range order (SRO) in the Pd−Au surface alloy (i.e., a preference for dissimilar metal atoms as nearest neighbors).[58] The LEISS studies carried out in our group for the 5 ML Pd/5 ML Au/Mo(110) alloy system showed the surface Pd concentration is only 18% after an anneal at 800 K for 20 min.[8,59] Therefore, both preferential surface segregation of Au and the chemical SRO lead to an exceptionally low number of larger Pd ensembles (e.g., Pd dimers, Pd trimers, and Pd patches, etc.) on the alloy surface. Consequently, the most probable surface ensemble is a Pd monomer surrounded by Au atoms. Maroun et al. recently reported similar Pd ensembles on the Pd/Au(111) surface could be synthesized using electrochemical methods.[28] On the basis of their IR and STM data, the critical surface ensemble for CO adsorption was identified as the Pd monomer. At low surface Pd concentration (7% and 15%), only an IR feature associated with linearly bound CO on the Pd monomer was observed. This feature increased in intensity up to 22% surface Pd at which coverage bridge-bound CO features begin to emerge.

Another obvious feature of Figure 5 is that the CO-IR intensity for the Au atop feature drops dramatically for the alloy surface. This is noteworthy in view of our previous LEISS study indicating that the 5 ML Pd/5 ML Au alloy system consists of 82% Au at the surface following an 800 K anneal.[8,59] Assuming this composition, the IR Au intensity for saturation CO on this alloy surface should be reduced by about 20%. However, a decrease of more than two-thirds is observed, indicating that the probability of CO adsorption on Au decreases substantially on the Pd−Au alloy surface. The preference of CO adsorption for isolated metal sites in bimetallic alloy systems has been observed previously.[60−62] For instance, for the Pt−Co alloy system with STM, Gauthier et al. found CO to adsorb exclusively on top of the Pt sites.[60] Also the IRAS study from Rutten et al. suggested that CO adsorption at atop Rh sites was preferred over Pt atop sites on a $Pt_{0.25}Rh_{0.75}$ single-crystal surface, even though the CO adsorption heats for Pt(111) and Rh(111) surfaces are very close.[62] It is reasonable to assume that a similar situation occurs for a Pd−Au alloy. Namely, CO adsorption on isolated Pd sites is enhanced, while that on Au is attentuated.[63]

The last key point remaining to be explained in Figure 5 is the CO frequency shift for the atop Pd feature, which moves from 2109 cm^{-1} on the pure Pd film to 2088 cm^{-1} on the alloy surface. This shift has been ascribed to the influence of a ligand effect.[30] Since the frequency shift is largely affected by the chemical interaction between the substrate and CO (mainly the back-donation of electrons from the metal d bands to CO $2\pi^*$ antibonding orbital), the addition of Au to the Pd surface alters the width and center of the Pd d bands and thus shifts the CO internal frequency.[31] Qualitatively, a linear relationship between the CO stretching frequency and the $2\pi^*$ occupation are applicable for CO on Pd.[31] Consequently, a continuous shift of the CO stretching frequency is anticipated when the surface Pd concentration is varied from bulk Pd to Pd−Au compositions with increasing amounts of Au. However, no such frequency shift is observed (see Figure 8A). Most likely, the other determining factor in the frequency shift, the vibrational coupling (or the dipole−dipole coupling), plays an important role. As mentioned earlier, a weak feature at 2086 cm^{-1} has been observed on both 10 ML Pd film and Pd(111) single-crystal surfaces. The frequency of this feature closely resembles that of isolated Pd sites on Pd−Au alloy surfaces, suggesting a similar chemical environment (Figure 6). With this consideration, the frequency shift on pure Pd surfaces to 2109 cm^{-1} at saturation CO coverage can be explained by a coverage-dependent frequency shift. At low CO coverages on Pd(111) facets, 3-fold hollow and 2-fold bridge sites are the energetically

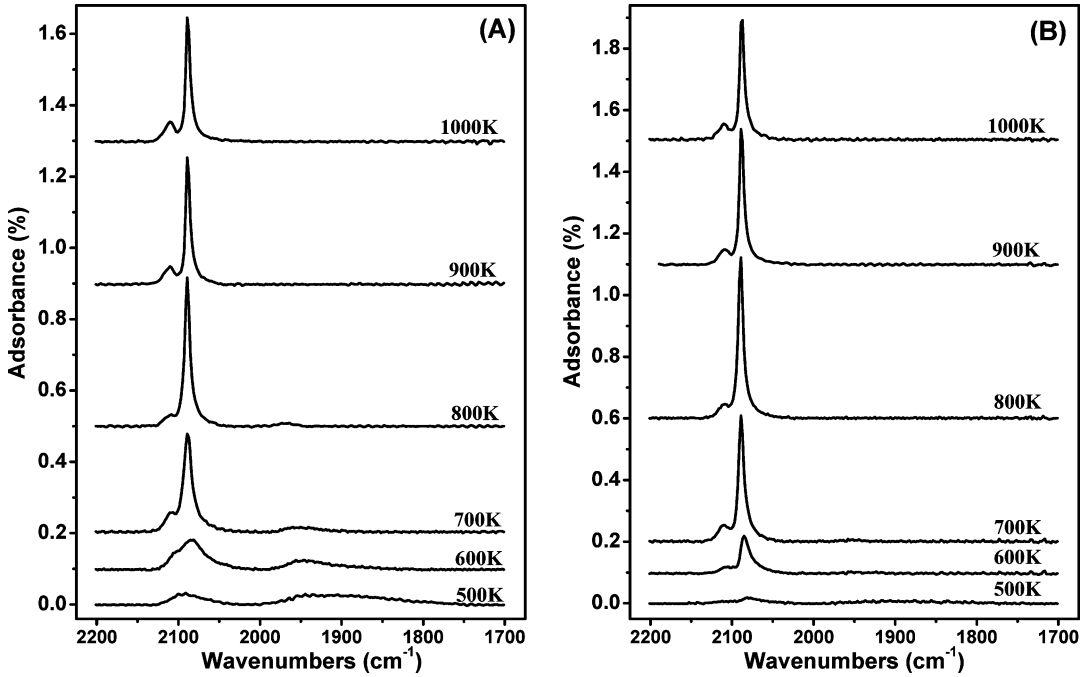

Figure 7. IRAS spectra for saturation CO coverages on (A) 7.5 ML Pd/2.5 ML Au/Mo(110) and (B) 2.5 ML Au/7.5 ML Pd/Mo(110) alloy films as a function of the sample annealing temperature. The sample was annealed for 20 min at each temperature, and the spectra were acquired at 80 K.

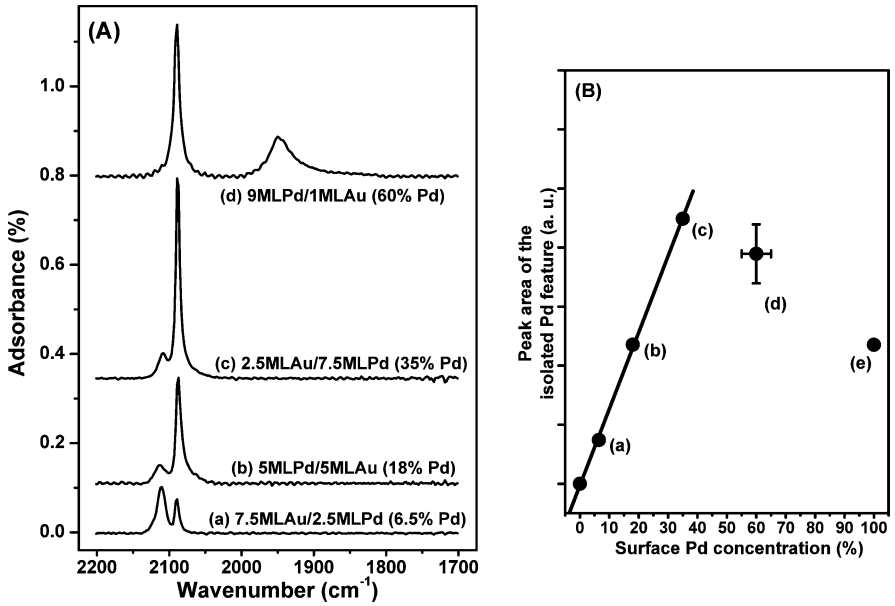

Figure 8. (A) IRAS spectra for CO adsorption on alloy films with different Pd to Au ratios. All the alloy films were annealed at 800 K for 30 min, and the spectra were acquired at 80 K with saturation CO coverage. (B) The integrated peak area for the isolated Pd feature as a function of the surface Pd concentration obtained from ref 8. Point e corresponds to the peak area of the CO Pd atop feature on 10 ML pure Pd film.

favorable adsorption sites; the minor feature for Pd atop sites appears only because of surface disorder. At this stage, the CO intermolecular distance is relatively large, so the repulsive interaction between CO molecules is negligible (Figure 6). However, at CO coverages higher than 0.5 ML, the condensed, highly ordered (2×2) structure forms. The CO molecules are crowded such that the repulsion force becomes dominant and shifts the frequencies of both the 3-fold hollow and atop features to higher values (Figure 6). Both these shifts are made in one step (from 2086 to 2109 cm^{-1} for Pd atop sites and from 1845 to 1892 cm^{-1} for Pd 3-fold hollow sites, see Figures 6 and 1), paralleling closely the CO overlayer structural change. These data support the argument that the frequency shift is caused primarily by dipole−dipole coupling, not by a chemical interaction mediated by the substrate. As mentioned above, the CO adsorption probability on Au is greatly reduced on the alloy surface. Most probably the Au atoms surrounding the isolated Pd sites likely do not adsorb CO. (A reduction of the overall CO coverage on the alloy surface has been confirmed by TPD experiments.[8]) Therefore, the dipole−dipole coupling is likely significantly attenuated on the alloy surface, reducing the magnitude of the CO blue-shift on the isolated Pd sites. Of interest is the insensitivity of the CO frequency on atop sites to the chemical interaction between the substrate and CO. Further experimental and theoretical work is needed to clarify this issue.

Alloy Films as a Model Alloy System. The data outlined above clearly show that lattice-matched alloy films grown on a refractory metal substrate can be used as a model alloy system for surface science and catalytic studies. Recent LEISS results from our group show that surface compositions for 10 ML thick

Pd−Au alloy films on Mo(110) with various Pd to Au ratios are in an excellent agreement with data from previous studies on polycrystalline bulk Pd−Au alloys.[8,16] Further ancillary work to confirm the efficiency of this thin film methodology has been carried out using IRAS experiments of CO adsorbed on Pd−Au alloy films with varying ratios annealed to the different temperatures.

Figure 7 displays CO-IRAS spectra for 7.5 ML Pd/2.5 ML Au (Figure 7A) and 2.5 ML Au/7.5 ML Pd (Figure 7B) alloy films on Mo(110) with different annealing temperatures. The alloy films were annealed at each temperature for 20 min, and all the spectra were acquired at 80 K with saturation CO coverage. These data give an excellent overview of the variations in the IR spectra as a function of annealing temperature for the same alloy composition with a different sequence of deposition. In both cases, low IR intensities and broad IR features have been observed after annealing the alloy films at relatively low temperatures (500 and 600 K), similar with the conditions shown earlier for the 5 ML Pd/5 ML Au case. However, clear differences are still apparent between these two sets of data, while IR spectra mainly present the characteristic features from the second-deposited metal, indicating the limited intermixing between Pd and Au after annealing at low temperatures. Subsequent to a 700 K anneal, the IR intensity begins to rise and the isolated Pd peak becomes the dominant feature. The IR intensity saturates after annealing at 800 K; however, the IR features are not well resolved until an annealing temperature between 900 and 1000 K. Apparently, the same stable alloy films are formed after annealing between 800 and 1000 K regardless of the deposition sequence. Yi et al. reported that the surface compositions of 5 ML Au/5 ML Pd alloy films on Mo(110) remain constant as $Au_{0.8}Pd_{0.2}$ after annealing between 700 and 1000 K independent of the metal deposition orders.[8] Therefore, on the basis of these LEISS and IRAS experiments, it is evident that a thermodynamic equilibrium is reached after annealing the Pd−Au alloy films to a sufficiently high temperature. Once reaching equilibrium, the LEISS data suggest Au preferentially enriches the alloy surface, and the IRAS data indicate a well-ordered surface morphology with isolated Pd sites.

As shown above, LEISS is a preferred technique for accessing the surface composition, but this technique is relatively insensitive to the surface morphology. On the other hand, IRAS using CO as a probe molecule provides detailed information about the surface morphology and adsorption sites but is lacking in quantitative analysis. Hence, in the literature there has been a history of using CO-IRAS to "titrate" the binary alloy surface composition. For instance, Varga's group compared the alloy surface concentrations obtained from LEISS and HREELS of CO adsorption results for $Pt_{25}Ni_{75}$(111) single-crystal alloy. These authors found that CO-HREELS is not generally appropriate for determining the surface composition to a high accuracy. Only under some favorable conditions (annealed over 1000 K, with comparably small number of surface defects) were the results from both methods in agreement.[64−67] The present study examines this possibility for Pd−Au alloy surfaces by combining CO-IRAS and LEISS results. Figure 8A summarizes CO-IRAS spectra for various Pd to Au bulk ratios, provided all the alloy films were annealed at 800 K for 30 min prior to the saturation CO adsorption at 80 K. The corresponding surface Pd concentration from LEISS results (ref 8) is listed along with the bulk ratio for each spectrum a−d in the figure. Clearly, 800 K is not high enough for 9 ML Pd/1 ML Au alloy film to obtain an ordered morphology. The isolated Pd feature on this surface is so broad that the Au atop feature cannot be well resolved. Also, the Pd multifold features are observed, as LEISS shows Pd is rich on this surface (60%). Ideally, the maximum amount of isolated Pd sites, without any adjacent Pd atoms, is 33.3% in an fcc<111> configuration. However, for 1:3, 1:1, and 3:1 Pd−Au mixtures (spectra a−c), annealing at 800 K does result in a well-ordered surface with isolated Pd as the main adsorption site. The intensity of the isolated Pd feature grows as the Pd bulk content increases, indicating that the concentration of isolated Pd surface sites can be systematically controlled by altering the bulk Pd to Au ratios. In Figure 8B, the integrated peak areas of the isolated Pd IR features are plotted as a function of the surface Pd concentration obtained from LEISS results (point e refers to the peak area of the CO Pd atop feature for 10 ML pure Pd film). An excellent linear relationship is apparent for the low surface Pd concentration up to 35% (spectra a−c), demonstrating that CO-IRAS can be used to monitor the isolated Pd concentration accurately within the low surface Pd concentration regime. As the most important adsorption sites on the alloy surface, the isolated Pd sites play critical roles in many catalytic reactions. The success in using CO-IRAS to titrate the isolated Pd is pivotal for establishing structure−reactivity relationships. The IR intensity becomes nonlinear at Pd-rich conditions (spectra d and e), probably because the vibrational coupling effect attenuates the IR intensity at high surface CO coverages. For CO adsorption on Ru(001) surfaces, Pfnur et al. reported a linear relationship between the surface CO coverage and the integrated IR intensity below $\theta_{CO} = 0.33$ ML. The IR intensity drops, thereafter, such that at saturation coverage the adsorption per adsorbed molecule is only 35−40% of the adsorption at $\theta_{CO} = 0.33$ ML. These authors ascribed this effect to the strong lateral interaction within the CO adlayer.[68] The excellent correlation between this study and our current work is further evidence that CO does not adsorb on the Au atoms that surround the isolated Pd. Hence, the dipole−dipole coupling effect is minimal in a Au-rich surface with Pd atoms isolated from each other.

4. Summary and Conclusion

CO chemisorptive properties on Pd, Au, and Pd−Au alloy films have been studied by infrared reflection−adsorption spectroscopy (IRAS). The 10 ML pure Pd and Au films on Mo(110) were found to have mainly flat and <111>-like facets with limited substrate influences. In order to address the alloying effects, the CO-IRAS spectra from Pd−Au alloy films have been compared with those of the corresponding single-component systems. A unique CO vibrational feature at 2088 cm^{-1} was identified as CO adsorbed on isolated Pd sites. The frequency shift of this feature has been ascribed mainly to dipole−dipole coupling, rather than to an electronic effect. After annealing the Pd−Au alloy films to relative high-temperature, highly ordered, thermodynamically stable alloy surfaces are observed. Au was found to enrich the surface and to further isolate the Pd atoms at equilibrium. Altering the bulk Pd to Au ratio can be used to control the isolated Pd concentration at the surface. More importantly, the concentration of isolated Pd surface sites can be measured by integrating the IR intensity of CO adsorbed at the isolated Pd sites.

Acknowledgment. The funding for this work was provided by the Department of Energy, Office of Basic Energy Sciences, Division of Chemical Sciences and Robert A. Welch Foundation. Fruitful discussions with M. S. Chen, C. W. Yi, and K. Luo are acknowledged.

References and Notes

(1) Rodriguez, J. A. *Surf. Sci. Rep.* **1996**, *24*, 223−287.
(2) Rodriguez, J. A.; Goodman, D. W. *Science* **1992**, *257*, 897.
(3) Besenbacher, F.; Chorkendorff, I.; Clausen, B. S.; Hammer, B.; Molenbroek, A. M.; Norskov, J. K.; Stensgaard, I. *Science* **1998**, *279*, 1913.
(4) Sachtler, J. W. A.; Van Hove, M. A.; Biberian, J. P.; Somorjai, G. A. *Phys. Rev. Lett.* **1980**, *45*, 1601.
(5) Han, Y. F.; Wang, J. H.; Kumar, D.; Yan, Z.; Goodman, D. W. *J. Catal.* **2005**, *232*, 467.
(6) Provine, W. D.; Mills, P. L.; Lerou, J. J. *Stud. Surf. Sci. Catal.* **1996**, *101*, 191.
(7) Stacchiola, D.; Calaza, F.; Burkholder, L.; Tysoe, W. T. *J. Am. Chem. Soc.* **2004**, *126*, 15384.
(8) Yi, C. W.; Luo, K.; Wei, T.; Goodman, D. W. *J. Phys. Chem. B* **2005**, *109*, 18335.
(9) Maehara, Y.; Kawanowa, H.; Gotoh, Y. *Surf. Rev. Lett.* **2003**, *10*, 425.
(10) Park, C.; Bauer, E.; Poppa, H. *Surf. Sci.* **1985**, *154*, 371.
(11) Payne, S. H.; Kreuzer, H. J.; Pavlovska, A.; Bauer, E. *Surf. Sci.* **1996**, *345*, L1.
(12) Gruzza, B.; Gillet, E. *Thin Solid Films* **1980**, *68*, 345.
(13) Pavlovska, A.; Paunov, M.; Bauer, E. *Thin Solid Films* **1985**, *126*, 129.
(14) Anton, R.; Eggers, H.; Veletas, J. *Thin Solid Films* **1993**, *226*, 39.
(15) Jablonski, A.; Overbury, S. H.; Somorjai, G. A. *Surf. Sci.* **1977**, *65*, 578.
(16) Swartzfager, D. G.; Ziemecki, S. B.; Kelley, M. J. *J. Vac. Sci. Technol.* **1982**, *19*, 185.
(17) Varga, P.; Hetzendorf, G. *Surf. Sci.* **1985**, *162*, 544.
(18) Kuntze, J.; Speller, S.; Heiland, W.; Deurinck, P.; Creemers, C.; Atrei, A.; Bardi, U. *Phys. Rev. B* **1999**, *60*, 9010.
(19) Kuntze, J.; Speller, S.; Heiland, W.; Atrei, A.; Rovida, G.; Bardi, U. *Phys. Rev. B* **1999**, *60*, 1535.
(20) Aschoff, M.; Speller, S.; Kuntze, J.; Heiland, W.; Platzgummer, E.; Schmid, M.; Varga, P.; Baretzky, B. *Surf. Sci.* **1998**, *415*, L1051.
(21) Nascente, P. A. P.; Decastro, S. G. C.; Landers, R.; Kleiman, G. G. *Phys. Rev. B* **1991**, *43*, 4659.
(22) Lee, Y. S.; Jeon, Y.; Chung, Y. D.; Lim, K. Y.; Whang, C. N.; Oh, S. J. *J. Korean Phys. Soc.* **2000**, *37*, 451.
(23) Weissman-Wenocur, D. L.; Stefan, P. M.; Pate, B. B.; Shek, M. L.; Lindau, I.; Spicer, W. E. *Phys. Rev. B* **1983**, *27*, 3308.
(24) Baddeley, C. J.; Ormerod, R. M.; Stephenson, A. W.; Lambert, R. M. *J. Phys. Chem.* **1995**, *99*, 5146.
(25) Gleich, B.; Ruff, M.; Behm, R. J. *Surf. Sci.* **1997**, *386*, 48.
(26) Piccolo, L.; Piednoir, A.; Bertolini, J. C. *Surf. Sci.* **2005**, *592*, 169.
(27) Baddeley, C. J.; Tikhov, M.; Hardacre, C.; Lomas, J. R.; Lambert, R. M. *J. Phys. Chem.* **1996**, *100*, 2189.
(28) Maroun, F.; Ozanam, F.; Magnussen, O. M.; Behm, R. J. *Science* **2001**, *293*, 1811.
(29) Chen, M. S.; Kumar, D.; Yi, C. W.; Goodman, D. W. *Science* **2005**, *310*, 291.
(30) Kugler, E. L.; Boudart M. *J. Catal.* **1979**, *59*, 201.
(31) Hoffmann, F. M. *Surf. Sci. Rep.* **1983**, *3*, 107.
(32) Ozensoy, E.; Goodman, D. W. *Phys. Chem. Chem. Phys.* **2004**, *6*, 3765.
(33) Kuhn, W. K.; Szanyi, J.; Goodman, D. W. *Surf. Sci. Lett.* **1992**, *274*, L611.
(34) Szanyi, J.; Kuhn, W. K.; Goodman, D. W. *J. Vac. Sci. Technol., A* **1993**, *11*, 1969.
(35) Guo, X.; Yates, J. T. *J. Chem. Phys.* **1989**, *90*, 6761.
(36) Ruggiero, C.; Hollins, P. *J. Chem. Soc., Faraday Trans.* **1996**, *92*, 4829.
(37) Jugnet, Y.; Cadete Santos Aires, F. J.; Deranlot, C.; Piccolo, L.; Bertolini, J. C. *Surf. Sci.* **2002**, *521*, L639.
(38) Meier, D. C.; Bukhtiyarov, V.; Goodman, D. W. *J. Phys. Chem. B* **2003**, *107*, 12668.
(39) Gottfried, J. M.; Schnidt, K. J.; Schroeder, S. L. M.; Christmann, K. *Surf. Sci.* **2003**, *536*, 206.
(40) Leung, L.-W. H.; He, J.-W.; Goodman, D. W. *J. Chem. Phys.* **1990**, *93*, 8328.
(41) Campbell, R. A.; Goodman, D. W. *Rev. Sci. Instrum.* **1992**, *63*, 172.
(42) Meier, D. C.; Fizzi, V. A.; Granozzi, G.; Lai, X.; Goodman, D. W. *Langmuir* **2002**, *18*, 698.
(43) Meier, D. C.; Goodman, D. W. *J. Am. Chem. Soc.* **2004**, *126*, 1892.
(44) Mikkelsen, A.; Ouattara, L.; Lundgren, E. *Surf. Sci.* **2004**, *557*, 109.
(45) Rose, M. K.; Mitsui, T.; Dunphy, J.; Borg, A.; Ogletree, D. F.; Salmeron, M.; Sautet, P. *Surf. Sci.* **2002**, *512*, 48.
(46) Giebel, T.; Schaff, O.; Hirschmugl, C. J.; Fernandez, V.; Schindler, K. M.; Theobald, A.; Bao, S.; Lindsay, R.; Berndt, W.; Bradshaw, A. M.; Baddeley, C.; Lee, A. F.; Lambert, R. M.; Woodruff, D. P. *Surf. Sci.* **1998**, *406*, 90.
(47) Bourguignon, B.; Carrez, S.; Dragnea, B.; Dubost, H. *Surf. Sci.* **1998**, *418*, 171.
(48) Ozensoy, E.; Meier, D. C.; Goodman, D. W. *J. Phys. Chem. B* **2002**, *106*, 9367.
(49) Rainer, D. R.; Wu, M.-C.; Mahon, D. I.; Goodman, D. W. *J. Vac. Sci. Technol., A* **1996**, *14*, 1184.
(50) Wei, T.; Goodman, D. W. Manuscript in preparation.
(51) Xu, C.; Goodman, D. W. *Surf. Sci.* **1996**, *360*, 249.
(52) Chen, M. S.; Cai, Y.; Yan, Z.; Goodman, D. W. *J. Am. Chem. Soc.* **2006**, *128*, 6341−6346.
(53) Shih, H. D.; Bauer, E.; Poppa, H. *Thin Solid Films* **1982**, *88*, L21.
(54) Bennett, R. A.; Poulston, S.; Price, N. J.; Reilly, J. P.; Stone, P.; Barnes, C. J.; Bowker, M. *Surf. Sci.* **1999**, *816*, 433−435.
(55) Aaen, A. B.; Lagsgaard, E.; Ruban, A. V.; Stensgaard I. *Surf. Sci.* **1998**, *408*, 43.
(56) Sellidj, A.; Koel, B. E. *Phys. Rev. B* **1994**, *49*, 8367.
(57) Ruff, M.; Frey, S.; Gleich, B.; Behm, R. J. *Appl. Phys. A* **1998**, *66*, S513.
(58) Sadigh, B.; Asta, M.; Ozolins, V.; Schmid, A. K.; Bartelt, N. C.; Quong, A. A.; Hwang, R. Q. *Phys. Rev. Lett.* **1999**, *83*, 1379.
(59) Luo, K.; Wei, T.; Yi, C. W.; Axnanda, S.; Goodman, D. W. *J. Phys. Chem. B* **2005**, *109*, 23517.
(60) Gauthier, Y.; Schmid, M.; Padovani, S.; Lundgren, E.; Bus, V.; Kresse, G.; Redinger, J.; Varga, P. *Phys. Rev. Lett.* **2001**, *87*, 036103.
(61) Engelhardt, M. P.; Schmid, M.; Biedermann, A.; Denecke, R.; Steinruck, H. P.; Varga, P. *Surf. Sci.* **2005**, *578*, 124.
(62) Rutten, F. J. M.; Nieuwenhuys, B. E.; McCoustra, M. R. S.; Chesters, M. A.; Hollins, P. *J. Vac. Sci. Technol., A* **1997**, *15*, 1619.
(63) Wei, T.; Goodman, D. W. Manuscript in preparation.
(64) Schmid, M.; Stadler, H.; Varga, P. *Phys. Rev. Lett.* **1993**, *70*, 1441.
(65) Weigand, P.; Hofer, W.; Varga, P. *Surf. Sci.* **1993**, *350*, 287−288.
(66) Pantforder, A.; Skonieczny, J.; Janssen, E.; Meister, G.; Goldmann, A.; Varga, P. *Surf. Sci.* **1995**, *337*, 177.
(67) Pantforder, A.; Skonieczny, J.; Janssen, E.; Meister, G.; Goldmann, A.; Varga, P. *Surf. Sci.* **1995**, *824*, 331−333.
(68) Pfnur, H.; Menzel, D.; Hoffmann, F. M.; Ortega, A.; Bradshaw, A. M. *Surf. Sci.* **1980**, *93*, 431.
(69) Zellner, M. B.; Goda, A. M.; Skoplyak, O.; Barteau, M. A.; Chen, J. G. *Surf. Sci.* **2005**, *583*, 281.